Atomic and electronic structure of the K/Si(111)$\sqrt{3}\times\sqrt{3}R30^{\circ}$-*B* chemisorption system

H. Q. Shi, M. W. Radny, and P. V. Smith*
School of Mathematical and Physical Sciences, The University of Newcastle, Callaghan, Australia, 2308
(Received 17 November 2003; revised manuscript received 11 August 2004; published 20 December 2004)

Ab initio plane-wave pseudopotential density functional theory (DFT) calculations have been carried out to determine the atomic and electronic structure of the K/Si(111)$\sqrt{3}\times\sqrt{3}R30^{\circ}$-*B* adsorption system at 1/3 monolayer coverage. Chemisorption of the potassium atoms has been found to leave the topology and bonding structure of the Si(111)$\sqrt{3}\times\sqrt{3}R30^{\circ}$-*B* substrate essentially unchanged. The results also show that the lowest-energy K/Si(111)$\sqrt{3}\times\sqrt{3}R30^{\circ}$-*B* structures are very similar to the most energetically favorable geometries for the K/Si(111)7×7 chemisorption system. The minimum energy configuration has been found to be a structure in which the potassium atoms are positioned near the hollow H_3 sites, the boron atoms occupy the subsurface S_5 positions, and the silicon adatoms are located at the T_4 sites. The electronic structure of this lowest-energy K/Si(111)$\sqrt{3}\times\sqrt{3}R30^{\circ}$-*B* configuration has been found to be metallic.

DOI: 10.1103/PhysRevB.70.235325 PACS number(s): 68.35.Bs, 68.43.−h, 73.20.−r

I. INTRODUCTION

Alkali-metal- (AM-) silicon chemisorption systems provide ideal prototype systems for studying metal-semiconductor adsorbate systems. This is because AM atoms are monovalent and hence there is a high probability that stable, single bonds between the adatoms and substrate silicon atoms will be formed. Despite, however, the relative simplicity of AM-silicon systems and the large amount of research that has been devoted to them, a comprehensive understanding of the most stable atomic configurations and their associated interactions and bonding characteristics still remains to be achieved.

The most widely studied alkali metal on silicon surfaces has been potassium. Most of these studies have focused on the Si(001)−K chemisorption system[1–18] and comparatively little work has been devoted to the interaction of potassium with the (111) surfaces of silicon. It is well known that the most stable reconstruction of the ideal Si(111)1×1 surface is the Si(111)7×7 surface. When boron atoms are chemisorbed on the Si(111) surface at 1/3 monolayer (ML) coverage, however, a Si(111)$\sqrt{3}\times\sqrt{3}R30^{\circ}$-*B* reconstruction is observed. Both the experimental data[19–21] and theoretical calculations[20–22] suggest that the boron atoms within this $\sqrt{3}\times\sqrt{3}R30^{\circ}$ reconstructed surface are chemisorbed at the subsurface S_5 sites—that is, at the fourfold-coordinated second-layer sites directly below the silicon adatoms sitting at the threefold coordinated T_4 surface positions. Since the boron atoms are chemisorbed below the surface, the local atomic structure of the Si(111)$\sqrt{3}\times\sqrt{3}R30^{\circ}$-*B*($S_5$) reconstructed surface is very similar to the Si adatom topology of the Si(111)7×7 surface. The electronic structures of these two surface topologies, however, are substantially different. Moreover, in contrast to the clean Si(111)7×7 surface, the Si(111)$\sqrt{3}\times\sqrt{3}R30^{\circ}$-*B*($S_5$) substrate should be chemically inert as there is no charge left on the dangling bond of the Si adatom at the T_4 site.[23] These observations suggest that somewhat different behavior might result from the chemisorption of potassium onto these two semiconducting surfaces.

The energetics of stable atomic structures for the K/Si(111)7×7 chemisorbed surface was investigated by Cho and Kaxiras.[24] Based on *ab initio* total-energy calculations they found that the Si adatom and rest atom on-top dangling bond sites were the highest-energy adsorption sites and that the high-coordination hollow sites were more stable by 0.83 eV and 0.34 eV, respectively. Similar behavior for potassium chemisorption on the ideal Si(111)1×1 surface was reported by Huaxiang and Ling[25] who found that the high coordination T_4 and H_3 hollow sites (above the fourth-layer silicon atoms) were approximately 0.3 eV more stable than the dangling bond on-top sites. Recent Scanning tunneling microscopy (STM) studies of Na adsorption on the Si(111)7×7 surface have revealed that at low coverage the Na adatoms are invisible to STM, although the adsorption enhances the brightness of the Si adatoms.[26] This has been explained by rapid diffusion of the Na adatoms resulting in an averaging of the STM image.[26] This interpretation was based on *ab initio* total-energy calculations which predicted that the lowest-energy sites for the Na adatoms on the Si(111)7×7 surface were located in the "basins" surrounding the rest atoms, analogous to the results obtained for the K/Si(111)7×7 system by Cho and Kaxiras.[24]

High-resolution core-level x-ray photoemission studies by Ma *et al.*[27] of potassium chemisorption on the Si(111)$\sqrt{3}\times\sqrt{3}R30^{\circ}$-*B* surface have shown a large core-level shift of ~1.2 eV for both the B(1*s*) and Si(2_p) states. The authors interpreted these large shifts in terms of a significant charge transfer from the potassium atoms to the Si-substrate dangling-bond state. Grehk *et al.*[28] studied the case of a submonolayer coverage of potassium on the Si(111)$\sqrt{3}\times\sqrt{3}R30^{\circ}$-*B* surface using angle-resolved photoelectron spectroscopy and found that deposition of potassium leads to the formation of a localized electronic state 0.7 eV below the Fermi level. The energy position of this state was also found to exhibit little dependence on the actual potassium coverage. Angle-resolved photoemission studies of the K/Si(111)7×7 and K/Si(111)$\sqrt{3}\times\sqrt{3}R30^{\circ}$-*B* interfaces by Weitering *et al.*[29,30] indicated that both systems are semiconducting at room temperature and saturation coverage. A dis-

persionless K-induced surface state was observed to occur below the Fermi level for both surfaces. Weitering *et al.*[29,30] also carried out low-energy electron diffraction (LEED) studies of the K/Si(111)$\sqrt{3}\times\sqrt{3}R30^{\circ}$-*B* surface and found that the $\sqrt{3}\times\sqrt{3}R30^{\circ}$ reconstruction persisted following chemisorption of the potassium. Based on these data and the angle-resolved ultraviolet photoemission spectroscopy (ARUPS) electronic structure which indicated that their observed back-bond surface state on the $\sqrt{3}\times\sqrt{3}R30^{\circ}$ potassium-chemisorbed surface was the same as for the clean Si(111)$\sqrt{3}\times\sqrt{3}R30^{\circ}$-*B* surface, they concluded that the potassium atoms were most likely bonded directly to the dangling-bond orbitals of the silicon adatoms.

To the best of our knowledge there have been no theoretical studies carried out to determine the atomic and electronic structure of the K/Si(111)$\sqrt{3}\times\sqrt{3}R30^{\circ}$-*B* chemisorption system. The goal of this paper is to report the results of accurate first-principles density functional theory (DFT) calculations of this system at 1/3 ML coverage. It will be shown that the minimum-energy structure corresponds to the potassium atoms chemisorbing at the high-coordination H_3 hollow sites rather than being singly bonded to the silicon adatoms at the T_4 sites. The electronic structure of this minimum-energy structure has also been calculated and shown to be metallic.

II. METHOD AND PROCEDURE

All of the calculations have been carried out using the *ab initio* total-energy and molecular dynamics program VASP (Vienna *ab initio* simulation package) which is based on the DFT pseudopotential plane-wave method.[31–33] Fully spin-polarized calculations have been performed using both ultrasoft (US) and PAW pseudopotentials[34] for all of the component atoms within the periodic slab unit cell. The Kohn-Sham equations have been solved using six special **k** points in the irreducible symmetry element of the surface Brillouin zone (SBZ) of the Si(111)$\sqrt{3}\times\sqrt{3}R30^{\circ}$ surface unit cell (SUC) and employing plane waves with kinetic energies up to ~20 Ry. Our periodic slab consisted of eight layers of silicon, together with hydrogen atoms below the bottom layer silicon atoms to saturate the bulk dangling bonds, and a vacuum region of ~20Å. The top four layers of the slab plus the chemisorbed potassium atoms were allowed to vary, and the minimum-energy structure was found by minimizing the forces using the Hellmann-Feynman theorem. The band structure for each optimized structure was obtained by calculating the energy eigenvalues along the main symmetry directions of the SBZ. The nature of the various electronic states was determined by calculating their associated charge and probability density distributions and *spd*-site-projected wave function character using the VASP program.[31–33]

III. RESULTS AND DISCUSSION

A. Atomic structure

Assuming, in accordance with the experiments, that the $\sqrt{3}\times\sqrt{3}R30^{\circ}$ reconstruction is retained after K chemisorption on the Si(111)$\sqrt{3}\times\sqrt{3}R30^{\circ}$-*B* surface, we have performed total-energy geometry optimization calculations for a variety of possible positions for the boron and potassium atoms within the Si(111)$\sqrt{3}\times\sqrt{3}R30^{\circ}$ SUC. Six structures were found to be stable. In each case, the lowest-energy structure corresponded to an equal number of up and down-spin electrons so that the net magnetic moment is zero. The relative total energies of these six structures are given in Table I, and the corresponding optimized geometries are presented in Figs. 1–6. The details of the geometries for the three lowest-energy structures are given in Tables II and III. These results

TABLE I. Total energies (in eV) of the six optimized K/Si(111)$\sqrt{3}\times\sqrt{3}R30^{\circ}$-*B* chemisorption structures relative to the energy of the K(T_1)Si(T_4)B(S_5) topology, obtained using ultrasoft (US) and PAW pseudopotentials.

Structure	ΔE (US)	ΔE (PAW)
K(H_3)Si(T_4)B(S_5)	−0.949	−0.973
K(T_4')Si(T_4)B(S_5)	−0.842	−0.874
K(T_4)Si(T_4')B(S_5)	−0.072	−0.134
K(T_1)Si(T_4)B(S_5)	0	0
K(H_3)Si(S_5)B(T_4)	0.496	0.459
K(T_1)Si(S_5)B(T_4)	0.854	0.822

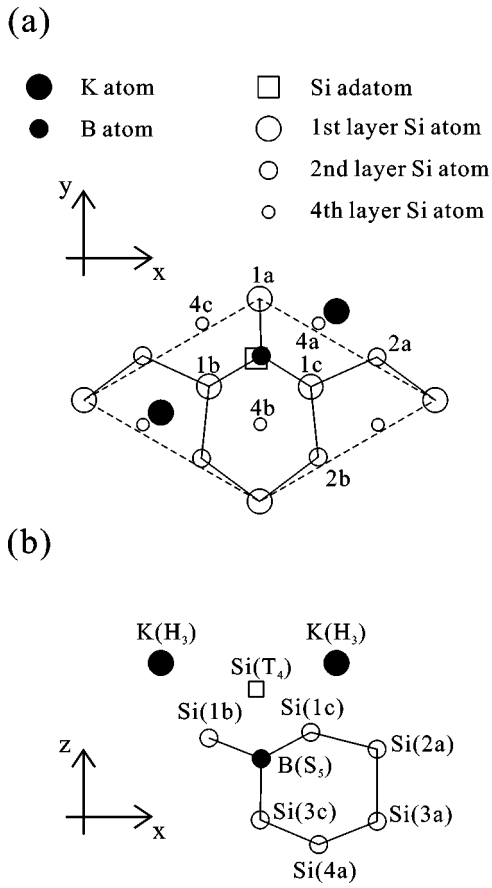

FIG. 1. Top (a) and side (b) views of our minimum-energy structure for the K/Si(111)$\sqrt{3}\times\sqrt{3}R30^{\circ}$-*B* chemisorption system for 1/3 ML coverage. As in all subsequent figures, the $\sqrt{3}\times\sqrt{3}R30^{\circ}$ surface unit cell is indicated by the dashed lines.

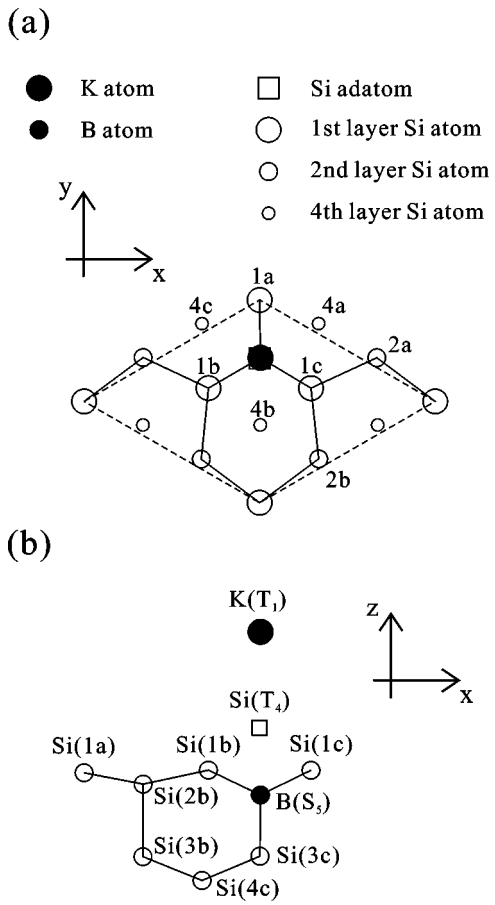

FIG. 2. Top (a) and side (b) views of the $K(T_1)Si(T_4)B(S_5)$ structure of the $K/Si(111)\sqrt{3}\times\sqrt{3}R30^{\circ}$-*B* chemisorption system for 1/3 ML coverage.

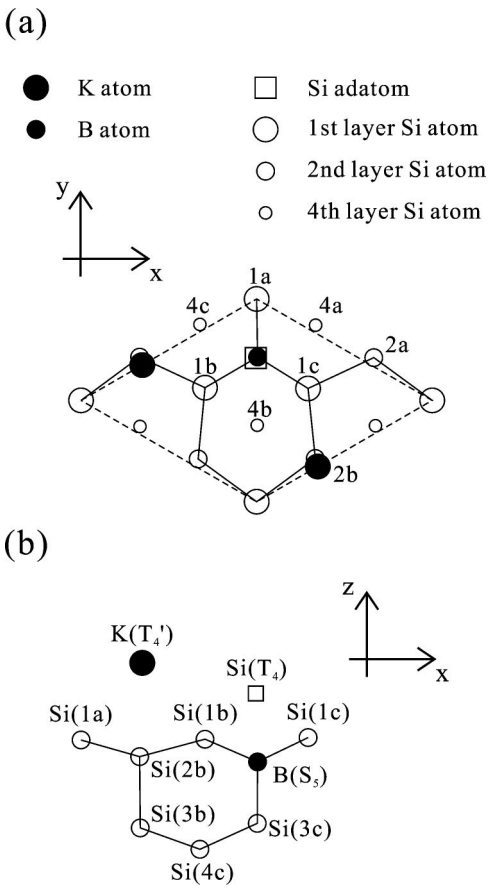

FIG. 3. Top (a) and side (b) views of the $K(T_4')Si(T_4)B(S_5)$ structure of the $K/Si(111)\sqrt{3}\times\sqrt{3}R30^{\circ}$-*B* chemisorption system for 1/3 ML coverage.

have been obtained using both US and PAW pseudopotentials. As the values obtained from both pseudopotentials are very similar, only the PAW results will be discussed in the following text.

The two lowest-energy structures have been found to retain the topology of the substrate after chemisorption of the potassium atoms. The structure shown in Fig. 1 was found to be most energetically stable. In this configuration, the boron atoms replace the silicon atoms sitting at the subsurface S_5 sites, the silicon atoms occupy the T_4 adatom sites, and the potassium atoms chemisorb in the vicinity of the H_3 hollow sites $[K(H_3)Si(T_4)B(S_5)]$. The energy of this structure has been found to be 0.97 eV lower in energy than the on-top $K(T_1)Si(T_4)B(S_5)$ structure shown in Fig. 2. This latter structure was suggested by Weitering *et al.*[29,30] as the most likely structure for the $K/Si(111)\sqrt{3}\times\sqrt{3}R30^{\circ}$-*B* chemisorption system at 1/3 ML coverage. The $K(H_3)Si(T_4)B(S_5)$ minimum-energy structure is very similar to the second lowest stable structure found by Cho and Kaxiras[24] for the $K/Si(111)7\times7$ system in which the K adatom is also chemisorbed near the H_3 hollow site. Interestingly, the energy for the case in which the K adatom is chemisorbed directly above the Si adatom at the T_1 site of the $Si(111)7\times7$ surface was found by Cho and Kaxiras to be 0.83 eV higher than for K chemisorption near the H_3 hollow site. This is quite close to our value of 0.97 eV obtained for the $K(T_1)Si(T_4)B(S_5)$ structure on the $K/Si(111)\sqrt{3}\times\sqrt{3}R30^{\circ}$-*B* surface.

Our second lowest-energy structure is the $K(T_4')Si(T_4)B(S_5)$ geometry shown in Fig. 3. In this structure, the boron atoms sit at the subsurface S_5 sites, the silicon surface atoms occupy the T_4 sites, and the potassium atoms are chemisorbed close to the T_4' threefold-coordinated sites which are positioned directly above the second-layer silicon atoms. These latter sites are equivalent to the T_4 sites occupied by the silicon adatoms. The $K(T_4')Si(T_4)B(S_5)$ structure is 0.10 eV less stable than our minimum-energy $K(H_3)Si(T_4)B(S_5)$ topology but 0.87 eV more stable than the on-top $K(T_1)Si(T_4)B(S_5)$ configuration. A very similar T_4-like K-adatom structure has also been discussed by Cho and Kaxiras[24] for the $K/Si(111)7\times7$ surface. In fact, this structure was found to be the most stable geometry for the $K/Si(111)7\times7$ chemisorption system with an energy 0.02 eV lower per 7×7 SUC than that for the H_3 hollow site topology.

Calculated values for some of the atomic relaxations and bond lengths of our lowest-energy $K(H_3)Si(T_4)B(S_5)$ structure and the clean $Si(111)\sqrt{3}\times\sqrt{3}R30^{\circ}$-*B* surface are presented in Table II. It is also interesting to compare the geometry of our minimum-energy $K(H_3)Si(T_4)B(S_5)$ structure with that of our second lowest-energy configuration

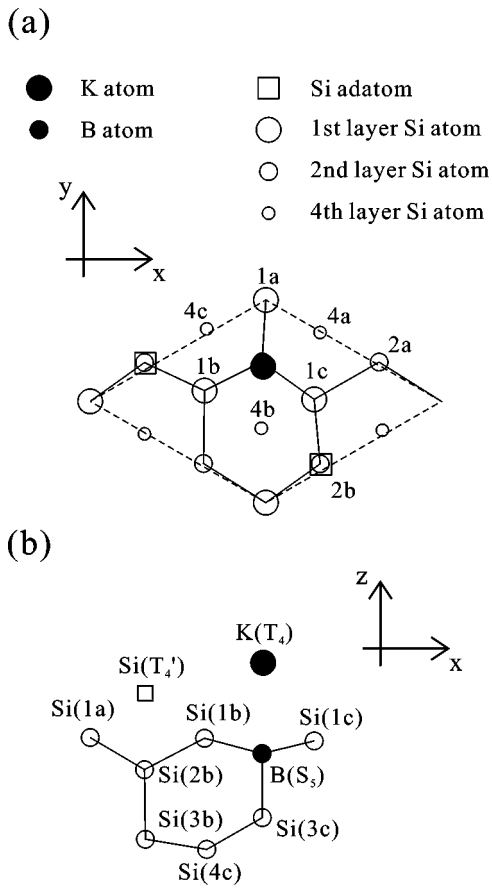

FIG. 4. Top (a) and side (b) views of the $K(T_4)Si(T_4')B(S_5)$ structure of the $K/Si(111)\sqrt{3}\times\sqrt{3}R30^{\circ}$-*B* chemisorption system for 1/3 ML coverage.

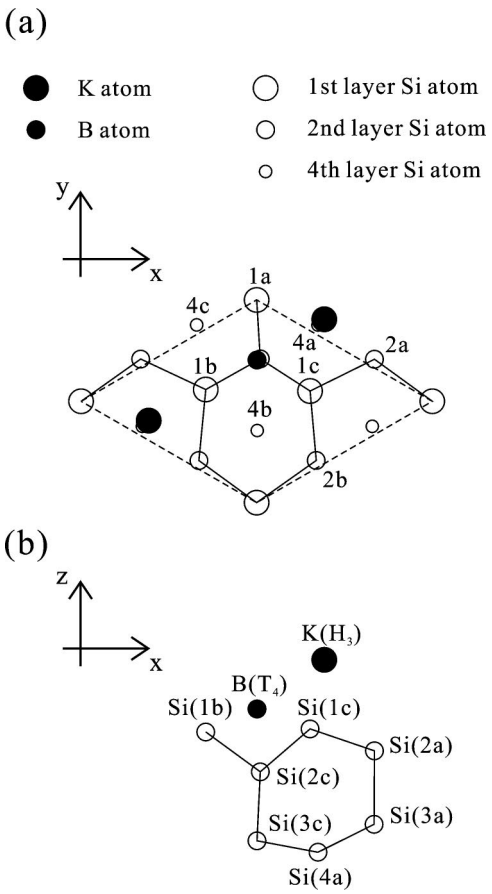

FIG. 5. Top (a) and side (b) views of the $K(H_3)Si(S_5)B(T_4)$ structure of the $K/Si(111)\sqrt{3}\times\sqrt{3}R30^{\circ}$-*B* chemisorption system for 1/3 ML coverage.

$[K(T_4')Si(T_4)B(S_5)]$. These data are presented in Table III. The distances between the subsurface $B(S_5)$ atom and the underlying third-layer silicon atom for these two structures are almost the same at 2.00 Å and 2.01 Å, respectively. Both of these values are fairly close to the value of 1.98 Å for the same bond length on the clean $Si(111)\sqrt{3}\times\sqrt{3}R30^{\circ}B$ surface (see Table II). The bond lengths between the $B(S_5)$ atom and the three neighboring first-layer silicon atoms are also quite similar for these two structures and were determined to be 2.01 Å, 2.09 Å, and 2.09 Å $[K(H_3)Si(T_4)B(S_5)]$ and 2.03 Å, 2.12 Å, and 2.10 Å $[K(T_4')Si(T_4)B(S_5)]$. The corresponding distances for the $Si(111)\sqrt{3}\times\sqrt{3}R30^{\circ}$–*B* structure are 2.03 Å, 2.12 Å, and 2.08 Å. These data demonstrate that, for the two lowest-energy structures, the chemisorption of potassium on the $Si(111)\sqrt{3}\times\sqrt{3}R30^{\circ}$-*B* surface does not significantly change the topology of the substrate. These results are consistent with the experimental data of Weitering *et al.*[29,30] who found that the backbond surface state which they observed on the $\sqrt{3}\times\sqrt{3}R30^{\circ}$ K-chemisorbed surface was essentially the same as for the $Si(111)\sqrt{3}\times\sqrt{3}R30^{\circ}$-*B* surface. Similar conclusions were obtained by Ma *et al.*[27] from their high-resolution core-level photoemission measurements.

The surface topologies of these two lowest-energy configurations are, however, clearly different to that of the clean surface. The silicon adatoms at the T_4 sites of both structures are determined to be 0.22 Å higher than the adatoms on the clean $Si(111)\sqrt{3}\times\sqrt{3}R30^{\circ}$-*B* surface.[23] The distances between the $Si(T_4)$ adatoms and the underlying $B(S_5)$ atoms of 2.28 Å and 2.23 Å for the $K(H_3)Si(T_4)B(S_5)$ and $K(T_4')Si(T_4)B(S_5)$ structures, respectively, are also longer than the corresponding distance of 2.18 Å for the clean $Si(111)\sqrt{3}\times\sqrt{3}R30^{\circ}$-*B* substrate. The average distance between each $Si(T_4)$ adatom and its three neighboring first layer silicon atoms is 2.44 Å for both structures, which is again longer than the corresponding distance of 2.36 Å for the clean $Si(111)\sqrt{3}\times\sqrt{3}R30^{\circ}$-*B* surface.[23] These observed changes in the $Si(T_4)$ bonding structure suggest that some charge is transferred from the potassium atom to the substrate. This is consistent with the high-resolution x-ray photoemission studies of Ma *et al.*[27] Similar results have been reported for the $Na/Si(111)7\times7$ chemisorption system where enhanced brightness of the Si adatoms in the filled-state STM images was attributed to charge transfer from the chemisorbed Na atoms to the neighboring Si adatoms.[26]

The vertical distances between the chemisorbed potassium atoms and the ideal positions of the first-layer silicon atoms for the $K(H_3)Si(T_4)B(S_5)$ and $K(T_4')Si(T_4)B(S_5)$ configurations are 2.05 Å and 2.20 Å, respectively. The bond lengths between each potassium atom and its three neighboring first layer silicon atoms are found to be asymmetric for

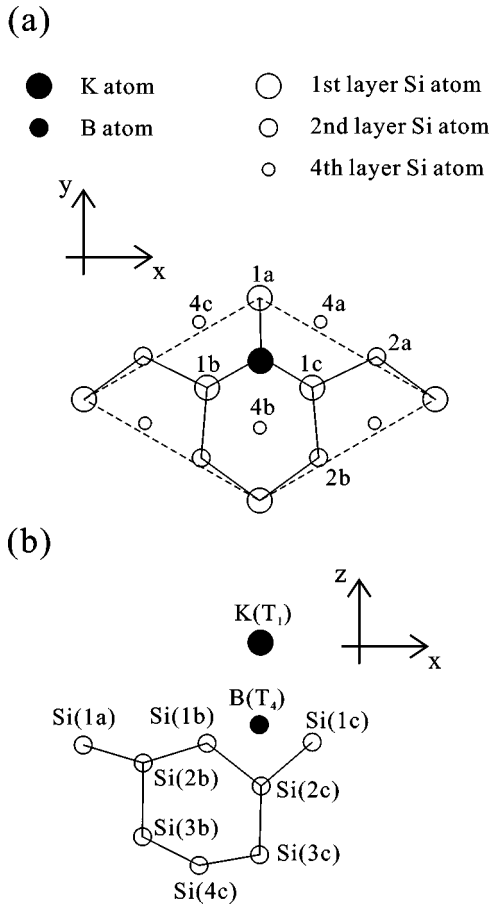

FIG. 6. Top (a) and side (b) views of the $K(T_1)Si(S_5)B(T_4)$ structure of the $K/Si(111)\sqrt{3}\times\sqrt{3}R30^{\circ}$-$B$ chemisorption system for 1/3 ML coverage.

the two structures and were predicted to be 3.47 Å, 3.03 Å, and 3.45 Å [$K(H_3)Si(T_4)B(S_5)$] and 3.41 Å, 3.31 Å, and 3.54 Å [$K(T_4')Si(T_4)B(S_5)$]. Moreover, the distance between each potassium atom and its nearest $Si(T_4)$ adatom for the $K(H_3)Si(T_4)B(S_5)$ structure is just 3.16 Å, while for the $K(T_4')Si(T_4)B(S_5)$ structure it is 3.81 Å. It is clear from these results that these minimum-energy structures prefer to form unequal bonds between each potassium atom and its neighboring silicon atoms.

In addition to these two lowest-energy structures and the $K(T_1)Si(T_4)B(S_5)$ on-top configuration, we have found three other structures that are energetically stable. In all three of these structures, there is significant reconstruction of the substrate. One of these structures corresponds to interchanging the Si adatoms and potassium atoms in the $K(T_4')Si(T_4)B(S_5)$ structure discussed above. This $K(T_4)Si(T_4')B(S_5)$ configuration, which is our third lowest-energy structure, is shown in Fig. 4. This topology has been found to be 0.13 eV more stable than the on-top $K(T_1)Si(T_4)B(S_5)$ topology, but 0.84 eV higher in energy than our minimum-energy $K(H_3)Si(T_4)B(S_5)$ topology shown in Fig. 1. Many of the relaxations and bond lengths of this $K(T_4)Si(T_4')B(S_5)$ configuration (which are also presented in Table III) are very similar to the corresponding values for the two lowest-energy $K(H_3)Si(T_4)B(S_5)$ and $K(T_4')Si(T_4)B(S_5)$ structures. In this geometry, however, the asymmetry of the K-Si (first-layer) bond lengths that we observed for the two lowest-energy structures has been significantly reduced with these bond lengths now being 3.27 Å, 3.22 Å, and 3.27 Å. The average distance between the $Si(T_4')$ adatom and the neighboring first-layer Si atoms of 2.61 Å is also 0.17 Å longer that the corresponding value for the two most stable structures. In addition, the boron atom is sitting much closer (~0.3 Å) to the surface and there is significantly more buckling in the second and third layers.

The other two stable structures that are characterized by significant reconstruction of the substrate have the boron atoms sitting at the T_4 adatom positions rather than occupying the subsurface S_5 sites. The $K(H_3)Si(S_5)B(T_4)$ structure, shown in Fig. 5, is 0.46 eV higher in energy than the on-top $K(T_1)Si(T_4)B(S_5)$ geometry. In this topology, the potassium and boron atoms sit at two different, but equivalent, threefold-coordinated sites, while the Si "adatoms" occupy the subsurface S_5 positions. The second structure $K(T_1)Si(S_5)B(T_4)$ is shown in Fig. 6. The total energy of this structure is 0.82 eV higher than the $K(T_1)Si(T_4)B(S_5)$ geometry. In this topology, the boron atoms again sit at the T_4 sites while the potassium atoms are located at the on-top T_1 sites. The fact that these two structures are significantly less stable than all of the $B(S_5)$ topologies is strong evidence that the boron atoms will remain at the subsurface S_5 sites following the chemisorption of potassium on the $Si(111)\sqrt{3}\times\sqrt{3}R30^{\circ}-B$ surface at 1/3 ML coverage.

B. Electronic structure

Electronic structure calculations have also been carried out for the three lowest-energy structures $K(H_3)Si(T_4)B(S_5)$, $K(T_4')Si(T_4)B(S_5)$ and $K(T_4)Si(T_4')B(S_5)$ that we have determined for the $K/Si(111)\sqrt{3}\times\sqrt{3}R30^{\circ}$-$B$ chemisorption system at 1/3 ML coverage. The energy bands obtained from calculating the eigenvalues in the vicinity of the energy gap for 20 **k** points along the $\Gamma-K-M-\Gamma$ symmetry directions of the $\sqrt{3}\times\sqrt{3}$ SBZ are shown in Figs. 7(a)–7(c). Also plotted for comparison in Fig. 7(d) is the electronic structure of the clean $Si(111)\sqrt{3}\times\sqrt{3}R30^{\circ}-B$ surface where the B atom also occupies the S_5 subsurface site.[23]

The extent of the contribution of the potassium adatoms to the various states of our lowest energy $K(H_3)Si(T_4)B(S_5)$ structure is indicated by the different sized circles in Fig. 7(a). The smallest solid circle represents a state to which each potassium adatom contributes at least 5% of the total charge, while the largest solid circle denotes a state where the potassium contribution is $\geqslant$40%. This information has been obtained from the *spd*-site-projected charge and probability densities provided by the VASP program. While the influence of the potassium adatoms is much more significant for the conduction-band states, as one would expect, we observe that there is an interaction with some of the valence-band states.

Comparison of the band structures of the three lowest-energy $K/Si(111)\sqrt{3}\times\sqrt{3}R30^{\circ}$-$B$ structures in Figs. 7(a)–7(c) shows that they have very similar valence-band

TABLE II. Atomic relaxations and bond lengths (in Å) of our optimized geometry for the K(H_3)Si(T_4)B(S_5) structure of the $K/\mathrm{Si}(111)\sqrt{3}\times\sqrt{3}R30^\circ$-$B$ chemisorption system for 1/3 ML coverage. The z coordinate is normal to the surface. The $z_{(\mathrm{K})}$ and $z_{\mathrm{Si}(A)}$ are defined relative to the z coordinate of the ideal first layer, and the $\Delta x_{(\mathrm{K})}$ and $\Delta y_{(\mathrm{K})}$ are defined relative to the ideal position of the underlying fourth-layer silicon atom. All of the Δz are with respect to the corresponding ideal silicon atom z values with the exception of $\Delta z_{\mathrm{Si}(A)}$ which is defined relative to the ideal adatom position assuming a Si-Si bond length of 2.33 Å. Values obtained from both theory and experiment for the $\mathrm{Si}(111)\sqrt{3}\times\sqrt{3}R30^\circ$-B($S_5$) configuration are also given for comparison.

	K(H_3)Si(T_4)B(S_5)		Si(111)$\sqrt{3}\times\sqrt{3}R30°$-B($S_5$)			
	US	PAW	Theory[a]	Expt.[b]	Expt.[c]	Expt.[d]
$Z_{(\mathrm{K})}$	2.03	2.05				
$\Delta x_{(\mathrm{K})}$	0.56	0.57				
$\Delta y_{(\mathrm{K})}$	0.40	0.40				
$z_{\mathrm{Si}(A)}$	1.17	1.20	0.98			
$\Delta z_{\mathrm{Si}(A)}$	0.39	0.42	0.21		0.25±0.1	
$\Delta z_{\mathrm{Si}(1a)}$	−0.33	−0.31	−0.45			
$\Delta z_{\mathrm{Si}(1b)}$	−0.42	−0.39	−0.38		−0.30±0.1	−0.17±0.2
$\Delta z_{\mathrm{Si}(1c)}$	−0.23	−0.21	−0.38			
Δz_{B}	−0.31	−0.30	−0.42		−0.50±0.1	
$\Delta z_{\mathrm{Si}(3a)}$	−0.02	−0.01	−0.04	0.0		
$\Delta z_{\mathrm{Si}(3b)}$	−0.02	−0.01	−0.03			
$\Delta z_{\mathrm{Si}(3c)}$	0.03	0.04	−0.08		−0.34±0.1	
$d_{\mathrm{K\text{-}Si}(1a)}$	3.46	3.47				
$d_{\mathrm{K\text{-}Si}(1b)}$	3.03	3.03				
$d_{\mathrm{K\text{-}Si}(1c)}$	3.46	3.45				
$d_{\mathrm{Si}(A)\text{-}\mathrm{Si}(1a)}$	2.46	2.46	2.38			
$d_{\mathrm{Si}(A)\text{-}\mathrm{Si}(1b)}$	2.39	2.40	2.35		2.336	
$d_{\mathrm{Si}(A)\text{-}\mathrm{Si}(1c)}$	2.45	2.45	2.36			
$d_{\mathrm{Si}(A)\text{-B}}$	2.27	2.28	2.18	2.14±0.13	2.320	
$d_{\mathrm{Si}(1a)\text{-B}}$	2.01	2.01	2.03			
$d_{\mathrm{Si}(1b)\text{-B}}$	2.09	2.09	2.12	2.21±0.13	2.154	
$d_{\mathrm{Si}(1c)\text{-B}}$	2.09	2.09	2.08			
$d_{\mathrm{Si}(3c)\text{-B}}$	1.99	2.00	1.98	1.98±0.04	2.190	
$d_{\mathrm{Si}(4)\text{-B}}$	3.55	3.56	3.50	3.53±0.09		
$z_{\mathrm{Si}(5)}$-z_{B}	5.13	5.14	5.02	5.20±0.20		
$z_{\mathrm{Si}(2)}$-z_{B}	0.31	0.315	0.405	0.49±0.35		
z_{B}-$z_{\mathrm{Si}(3)}$	2.04	2.04	1.945	1.90±0.16		

[a]Reference 23.
[b]Reference 36.
[c]Reference 37.
[d]Reference 38.

electronic structures. Moreover, the valence-band structures of these three structures are very similar to that of the clean $\mathrm{Si}(111)\sqrt{3}\times\sqrt{3}R30^\circ$-$B$ surface shown in Fig. 7(d). This is consistent with the observation of Grekh *et al.*[28] that the filled states are little affected by K adsorption. The most significant effect of the chemisorption of potassium on the valence-band structure of our two lowest-energy structures is an overall lowering in energy of the two occupied surface state bands along the K-M symmetry direction and to a progressively lesser extent, along the K-Γ and M-Γ symmetry directions. These states were shown in our earlier work on the clean $\mathrm{Si}(111)\sqrt{3}\times\sqrt{3}R30^\circ$-$B$ surface[23] to be well-localized backbond surface states involving strong bonding between the first-layer silicon atoms and the boron atoms at the S_5 subsurface sites. These states are indicated by the solid circles in Fig. 7(d). Two backbond surface state bands are also observed in the vicinity of the Γ point, the upper of which is a continuation of the K-M surface state bands and the second of which involves bonding between the Si(T_4) adatoms and the adjacent first-layer atoms. Detailed analysis of the nature of the wave functions for our lowest-energy structure for the K-chemisorbed surface has shown that these backbond surface states remain following K adsorption and are only shifted downward in energy by ~0.05 eV. These

TABLE III. Atomic relaxations and bond lengths (in Å) of the K(H_3)Si(T_4)B(S_5), K(T_4')Si(T_4)B(S_5), and K(T_4)Si(T_4')B(S_5) optimized structures for the K/Si(111)$\sqrt{3}\times\sqrt{3}R30°$-$B$ chemisorption system for 1/3 ML coverage. The definition of the various parameters is the same as in Table II.

	K(H_3)Si(T_4)B(S_5)		K(T_4')Si(T_4)B(S_5)		K(T_4)Si(T_4')B(S_5)	
	US	PAW	US	PAW	US	PAW
z_K	2.03	2.05	2.19	2.20	2.22	2.23
Δx_K	0.56	0.57	0.06	0.06	0.01	0.01
Δy_K	0.40	0.40	−0.19	−0.20	−0.11	−0.11
$z_{Si(A)}$	1.17	1.20	1.18	1.20	1.22	1.23
$\Delta z_{Si(A)}$	0.39	0.42	0.40	0.43	0.44	0.46
$\Delta z_{Si(1a)}$	−0.33	−0.31	−0.33	−0.31	−0.23	−0.21
$\Delta z_{Si(1b)}$	−0.42	−0.39	−0.31	−0.29	−0.26	−0.24
$\Delta z_{Si(1c)}$	−0.23	−0.21	−0.25	−0.23	−0.34	−0.32
Δz_B	−0.31	−0.30	−0.27	−0.25	0.02	0.04
$\Delta z_{Si(3a)}$	−0.02	−0.01	0.00	0.01	0.05	0.06
$\Delta z_{Si(3b)}$	−0.02	−0.01	−0.08	−0.07	−0.42	−0.42
$\Delta z_{Si(3c)}$	0.03	0.04	0.07	0.08	0.27	0.28
$d_{K\text{-}Si(1a)}$	3.46	3.47	3.54	3.41	3.28	3.27
$d_{K\text{-}Si(1b)}$	3.03	3.03	3.42	3.31	3.22	3.22
$d_{K\text{-}Si(1c)}$	3.46	3.45	3.31	3.54	3.23	3.27
$d_{Si(A)\text{-}Si(1a)}$	2.46	2.46	2.45	2.45	2.63	2.62
$d_{Si(A)\text{-}Si(1b)}$	2.39	2.40	2.42	2.43	2.59	2.58
$d_{Si(A)\text{-}Si(1c)}$	2.45	2.45	2.44	2.44	2.65	2.64
$d_{Si(A)\text{-}B}$	2.27	2.28	2.22	2.23		
$d_{K\text{-}B}$					2.98	2.97
$d_{Si(1a)\text{-}B}$	2.01	2.01	2.02	2.03	2.16	2.09
$d_{Si(1b)\text{-}B}$	2.09	2.09	2.12	2.12	2.08	2.16
$d_{Si(1c)\text{-}B}$	2.09	2.09	2.09	2.10	2.13	2.14
$d_{Si(3c)\text{-}B}$	1.99	2.00	2.00	2.01	2.09	2.09
$z_{Si(2a)}$-z_B	0.31	0.31	0.29	0.30	0.07	0.07
$z_{Si(2b)}$-z_B	0.31	0.32	0.18	0.17	−0.51	−0.52
z_B-$z_{Si(3a)}$	2.04	2.04	2.06	2.07	2.30	2.31
z_B-$z_{Si(3b)}$	2.04	2.04	2.15	2.15	2.78	2.80

results are entirely consistent with the angle-resolved x-ray photoemission experiments of Grekh *et al.*[28] on the K/Si(111)$\sqrt{3}\times\sqrt{3}R30^{\circ}$-$B$ surface which showed the occurrence of two backbond surface states close to the Γ point of the $\sqrt{3}\times\sqrt{3}$ SBZ about 1.9 eV and 2.2 eV below the Fermi energy. These backbond states, which they also observed for the clean Si(111)$\sqrt{3}\times\sqrt{3}R30°$-$B$ surface, were found to be largely unaffected by the K adsorption. Weitering *et al.*[29,30] also found a backbond state for the clean Si(111)$\sqrt{3}\times\sqrt{3}R30^{\circ}$-$B$ surface about 1.9 eV below the Fermi energy at the Γ point of the SBZ which persisted upon K adsorption. This surface state was predicted, however, to shift downward in energy by around 0.3 eV.[29,30] Charge density plots for the lower-energy backbond surface state of our lowest-energy K/Si(111)$\sqrt{3}\times\sqrt{3}R30^{\circ}$-$B$ structure are presented in Figs. 8(a) and 8(b).

Comparison of Figs. 7(a)–7(c) with Fig. 7(d) shows that the two lowest conduction-band states of the clean Si(111)$\sqrt{3}\times\sqrt{3}R30^{\circ}$-$B$ surface are shifted significantly downward in energy due to interaction with the potassium adatoms. These states are represented by the solid triangles and diamonds in Fig. 7(d) and correspond to surface states associated with the Si(T_4) adatom dangling bonds and coupling between the Si adatoms and the underlying boron atoms, respectively. The magnitude of the downward shift is clearly different for each of the three structures, however, with the energy gap between the resulting half-filled energy band and the next fully occupied band being 0.29 eV for the lowest-energy structure and 0.26 eV and 0.03 eV for the second and third lowest-energy structures, respectively. This is to be compared with the corresponding value of 0.61 eV for the clean Si(111)$\sqrt{3}\times\sqrt{3}R30^{\circ}$-$B$ surface. We also observe that the dispersion of the lowest-energy unoccupied band remains essentially unchanged following K adsorption at around 0.6 eV, while the dispersion of the second lowest conduction band is significantly reduced from 0.9 eV for the clean Si(111)$\sqrt{3}\times\sqrt{3}R30^{\circ}$-$B$ surface [Fig. 7(d)] to ~0.5 eV for the K-chemisorbed structures [Figs. 7(a)–7(c)]. Some of

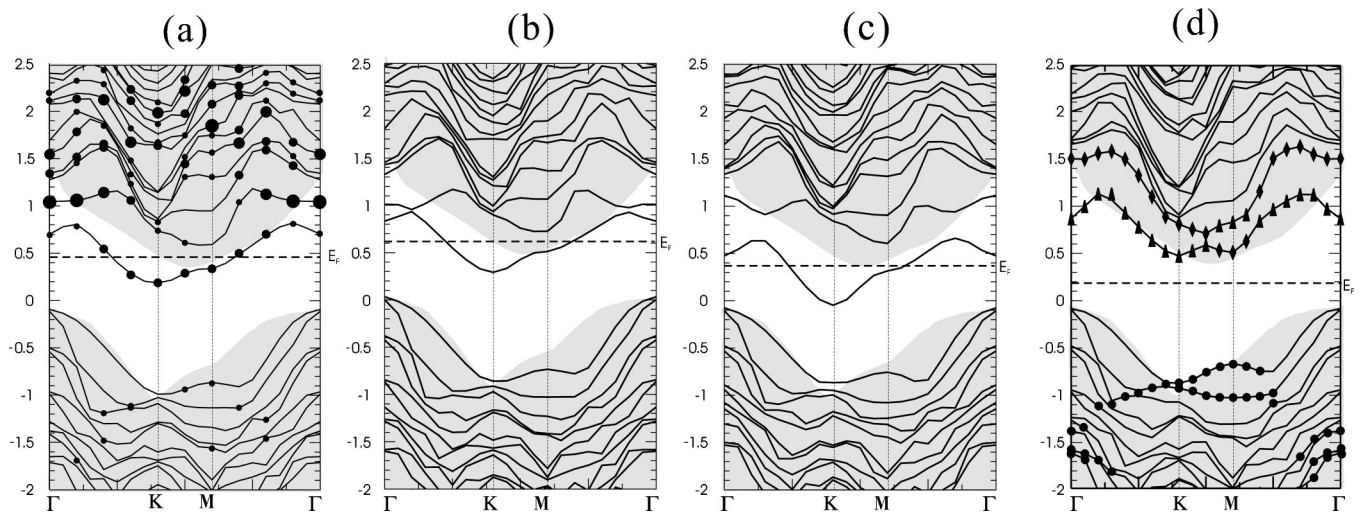

FIG. 7. Band structures for the (a) $K(H_3)Si(T_4)B(S_5)$, (b) $K(T_4')Si(T_4)B(S_5)$ and (c) $K(T_4)Si(T_4')B(S_5)$ configurations, and (d) the $Si(111)\sqrt{3}\times\sqrt{3}R30^{\circ}$-$B$ clean surface. The shaded regions represent the bulk-projected bandstructure. The solid circles in (a) denote the contribution of the potassium to the total charge of each state: • ⩾5%; ● ⩾10%; ● ⩾20%; ● ⩾40%. The solid triangles and diamonds in (d) denote the Si adatom dangling bond surface states, and surface states involving coupling between the silicon adatom and the underlying boron atoms, respectively. The solid circles in (d) indicate the occupied surface states.

the higher conduction-band states are also significantly affected by the presence of the potassium but the effect seems to be similar for all three structures. Figures 8(c) and 8(d) present probability density plots for the sixth fully empty state at the M point of the SBZ for the minimum-energy $K(H_3)Si(T_4)B(S_5)$ structure. It is clear that this state has a significant contribution from the K adatoms.

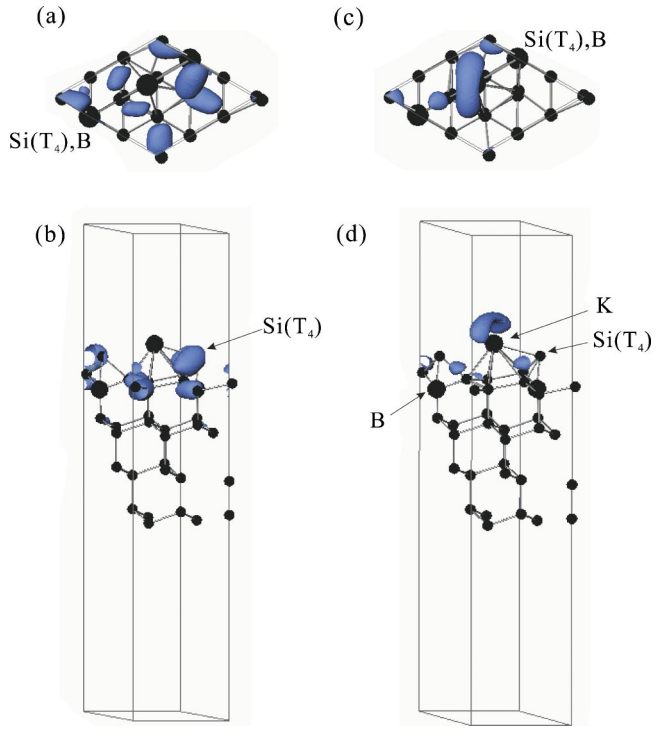

FIG. 8. (Color online) Top and side views of the density distributions for the lowest-energy backbond surface state at the Γ point [(a) and (b)] and the sixth conduction-band state at the M point of the $\sqrt{3}\times\sqrt{3}$ SBZ [(c) and (d)] for the $K(H_3)Si(T_4)B(S_5)$ structure. The isosurface values were 3.1×10^{-2} e/Å^3 for the Γ-point state and 2.5×10^{-2}Å^{-3} for the M-point state.

It is clear from Fig. 7(d) that the electronic structure of the clean $Si(111)\sqrt{3}\times\sqrt{3}R30^{\circ}$-$B$ surface is predicted to be semiconducting in agreement with experiment.[21,22] The electronic band structures of the three lowest-energy $K/Si(111)\sqrt{3}\times\sqrt{3}R30^{\circ}$-$B$ configurations, however, are all predicted to be metallic, contrary to the observations of both Grekh *et al.*[28] and Weitering *et al.*[29,30] [see Figs. 7(a)–7(c)]. This is due to the additional valence electron of each potassium adatom giving rise to an odd number of electrons per surface unit cell and hence partial filling of the spin-degenerate highest occupied energy band. For all three of our lowest-energy structures, the interaction between the potassium orbitals and the empty Si-adatom dangling-bond surface states of the clean $Si(111)\sqrt{3}\times\sqrt{3}R30^{\circ}$-$B$ surface has resulted in a half-filled band crossing the Fermi energy. This is consistent with the conclusion of Ma *et al.* that the large shifts observed in their Si(2p) and B(1s) core-level measurements are due to charge transfer from the K adatoms into the empty Si-substrate dangling-bond surface states.[27]

The photoelectron spectroscopy measurements of Grekh *et al.*[28] showed that the deposition of potassium at submonolayer coverages resulted in the formation of a state approximately 0.7 eV below the Fermi energy with an overall dispersion along the $\Gamma-M$ symmetry direction of the $\sqrt{3}\times\sqrt{3}$ SBZ of only 0.1 eV. The angle-resolved photoemission studies of Weitering *et al.*[29,30] also provided evidence for the occurrence of a relatively dispersionless K-induced surface state 0.65–0.85 eV below the Fermi energy. Moreover, this K-induced surface state was predicted to be a bonding combination of Si dangling bonds and K 4s orbitals.[29,30] As can be seen in Figs. 7(a)–7(c), our calculations provide no evidence for such a localized surface state. While our uppermost valence band does contain some contribution from the potas-

sium orbitals (along *K*-*M*), it involves coupling with the backbond surface states of the clean Si(111)$\sqrt{3}\times\sqrt{3}R30^{\circ}$-*B* surface rather than the Si(T_4) dangling-bond surface states. The only state close to E_F with the required character predicted by our calculations is the half-filled state which crosses the Fermi energy and it has an overall dispersion of 0.62–0.70 eV.

One way in which a system with an odd number of valence electrons per SUC can have a semiconducting band structure is for the uppermost occupied up or down-spin band to be fully occupied and nonoverlapping with any other band. Such a situation has, in fact, been found for a hemihydride Si-Si-H dangling-bond configuration on the Si(001) surface. In an attempt to obtain a semiconducting band structure for the K/Si(111)$\sqrt{3}\times\sqrt{3}R30^{\circ}$-*B* chemisorption system at 1/3 ML coverage we also carried out calculations for our minimum-energy K(H_3)Si(T_4)B(S_5) structure using the option in the VASP (Refs. 31–33) code to force the complete filling of the highest occupied up-spin band. These calculations also resulted in a metallic band structure.

IV. SUMMARY

The VASP plane-wave pseudopotential DFT code has been used to investigate the chemisorption of potassium on the Si(111)$\sqrt{3}\times\sqrt{3}R30^{\circ}$-*B* surface. The minimum-energy topology has been found to be the K(H_3)Si(T_4)*B*(S_5) structure. The K(T_1)Si(T_4)*B*(S_5) topology in which the potassium atoms sit at the T_1 sites directly above the Si adatoms at the T_4 sites was found to be less stable by 0.97 eV. Chemisorption structures involving potassium adsorption at the T_4 and T_4' sites were also found to be stable and lower in energy than the K(T_1) structure. These results demonstrate that the potassium atoms prefer to be located at threefold-coordinated sites where they form multiple bonds with the neighboring silicon atoms rather than forming single bonds with the silicon adatoms at the T_4 sites. This behavior is consistent with the results of Cho and Kaxiras for the K/Si(111)7×7 chemisorption system.[24] It is also consistent with the structure of solid KSi where the potassium atoms are found to sit at the threefold-coordinated positions directly above the centroids of the triangular faces of each Si_4 tetrahedral unit (Zintl ion), rather than be singly bonded directly above one of the vertices.[35] Two stable structures have also been found for the B atoms occupying the T_4 adatom positions instead of the S_5 second-layer site. The energy differences between these two structures and our minimum-energy K(H_3)Si(T_4)*B*(S_5) structure, however, were quite large (1.43 eV and 1.80 eV). The electronic structures of our three lowest-energy configurations for the K/Si(111)$\sqrt{3}\times\sqrt{3}R30^{\circ}$-*B* chemisorption system at 1/3 ML coverage were all predicted to be metallic rather than semiconducting as suggested by the photoemission experiments of Grekh *et al.*[28] and Weitering *et al.*[29,30] This may indicate, as suggested by these authors, that the K/Si(111)$\sqrt{3}\times\sqrt{3}R30^{\circ}$-*B* chemisorption system is a highly correlated system which requires going beyond the one-electron picture to obtain an accurate description of the electronic structure.

ACKNOWLEDGMENTS

This work was supported by a grant under the Merit Allocation Scheme on the National Facility of the Australian Partnership for Advanced Computing. H.Q.S. would like to thank the Australian Government and The University of Newcastle for financial support.

*Corresponding author. Electronic address: Phil.Smith@newcastle.edu.au

[1] T. Aruga, H. Tochihara, and Y. Murata, Phys. Rev. Lett. **53**, 372 (1984).
[2] I. P. Batra, J. M. Nicholls, and B. Reihl, J. Vac. Sci. Technol. A **5**, 898 (1987).
[3] L. Ye, A. J. Freeman, and B. Delley, Phys. Rev. B **39**, 10 144 (1989).
[4] R. Ramirez, Phys. Rev. B **40**, 3962 (1989).
[5] Y. Morikawa, K. Kobayashi, K. Terakura, and S. Blügel, Phys. Rev. B **44**, 3459 (1991).
[6] K. Kobayashi, Y. Morikawa, K. Terakura, and S. Blügel, Phys. Rev. B **45**, 3469 (1992).
[7] H. Q. Shi, M. W. Radny, and P. V. Smith, Surf. Sci. **561**, 215 (2004).
[8] R. Lindsay, H. Dürr, P. L. Wincott, I. Colera, B. C. Cowie, and G. Thornton, Phys. Rev. B **51**, 11 140 (1995).
[9] T. Abukawa and S. Kono, Phys. Rev. B **37**, 9097 (1988).
[10] E. G. Michel, P. Pervan, G. R. Castro, R. Miranda, and K. Wandelt, Phys. Rev. B **45**, 11 811 (1992).
[11] S. Tanaka, N. Takagi, N. Minami, and M. Nishijima, Phys. Rev. B **42**, 1868 (1990).
[12] T. Makita, S. Kohmoto, and A. Ichimiya, Surf. Sci. **242**, 65 (1991).
[13] A. J. Smith, W. R. Graham, and E. W. Plummer, Surf. Sci. **243**, L37 (1991).
[14] T. Abukawa, T. Kashiwakura, T. Okane, Y. Sasaki, H. Takahashi, Y. Enta, S. Susuki, S. Kono, S. Sato, T. Kinoshita, A. Kakizaki, T. Ishii, C. Y. Park, S. W. Yu, K. Sakamoto, and T. Sakamoto, Surf. Sci. **261**, 217 (1992).
[15] Y. Morikawa, K. Kobayashi, and K. Terakura, Surf. Sci. **283**, 377 (1993).
[16] H. Ishida and K. Terakura, Phys. Rev. B **40**, 11 519 (1989).
[17] P. Krüger and J. Pollmann, Appl. Phys. A: Solids Surf. **59**, 487 (1994).
[18] L. S. O. Johansson and B. Reihl, Phys. Rev. Lett. **67**, 2191 (1991).
[19] R. L. Headrick, I. K. Robinson, E. Vlieg, and L. C. Feldman, Phys. Rev. Lett. **63**, 1253 (1989).
[20] P. Bedrossian, R. D. Meade, K. Mortensen, D. M. Chen, J. A. Golovchenko, and D. Vanderbilt, Phys. Rev. Lett. **63**, 1257 (1989).
[21] I. W. Lyo, E. Kaxiras, and Ph. Avouris, Phys. Rev. Lett. **63**, 1261 (1989).

[22] E. Kaxiras, K. C. Pandey, F. J. Himpsel, and R. M. Tromp, Phys. Rev. B **41**, 1262 (1990).
[23] H. Q. Shi, M. W. Radny, and P. V. Smith, Phys. Rev. B **66**, 085329 (2002).
[24] K. Cho and E. Kaxiras, Surf. Sci. **396**, L261 (1998).
[25] F. Huaxiang and Y. Ling, Surf. Sci. **250**, L373 (1991).
[26] K. Wu, Y. Fujikawa, T. Nagao, Y. Hasegawa, K. S. Nakayama, Q. K. Xue, E. G. Wang, T. Briere, V. Kumar, Y. Kawazoe, S. B. Zhang, and T. Sakurai, Phys. Rev. Lett. **91**, 126101 (2003).
[27] Y. Ma, J. E. Rowe, E. E. Chaban, C. T. Chen, R. L. Headrick, G. M. Meigs, S. Modesti, and F. Sette, Phys. Rev. Lett. **65**, 2173 (1990).
[28] T. M. Grehk, L. S. O. Johansson, U. O. Karlsson, and A. S. Flodström, Phys. Rev. B **47**, 13 887 (1993).
[29] H. H. Weitering, J. Chen, N. J. DiNardo, and E. W. Plummer, Phys. Rev. B **48**, 8119 (1993).
[30] H. H. Weitering, J. Chen, R. Perez-Sandoz, and N. J. DiNardo, Surf. Sci. **307-9**, 978 (1994).
[31] G. Kresse and J. Hafner, Phys. Rev. B **47**, 558 (1993); **49**, 14 251 (1994).
[32] G. Kresse and J. Furthmüller, Comput. Mater. Sci. **6**, 15 (1996).
[33] G. Kresse and J. Furthmüller, Phys. Rev. B **54**, 11 169 (1996).
[34] G. Kresse and D. Joubert, Phys. Rev. B **59**, 1758 (1999).
[35] P. Villars and L. D. Calvert, *Pearson's Handbook of Crystallographic Data for Intermetallic Phases* (American Society for Metals, Metals Park, OH, 1985).
[36] P. Baumgartel, J. J. Paggel, M. Hasselblatt, K. Horn, V. Fernandez, O. Schaff, J. H. Weaver, A. M. Bradshaw, D. P. Woodruff, E. Rotenberg, and J. Denlinger, Phys. Rev. B **59**, 13 014 (1999).
[37] H. Huang, S. Y. Tong, J. Quinn, and F. Jona, Phys. Rev. B **41**, 3276 (1989).
[38] R. D. Meade and D. Vanderbilt, Phys. Rev. B **40**, 3905 (1989).